Pushing off the Walls: A Mechanism of Cell Motility in Confinement

R. J. Hawkins,[1] M. Piel,[2] G. Faure-Andre,[3] A. M. Lennon-Dumenil,[3] J. F. Joanny,[4] J. Prost,[4,5] and R. Voituriez[1]

[1]*UMR 7600, Université Pierre et Marie Curie/CNRS, 4 Place Jussieu, 75255 Paris Cedex 05 France*
[2]*UMR 144, Institut Curie/CNRS, 26 rue d'Ulm 75248 Paris Cedex 05 France*
[3]*U 653, Inserm/Institut Curie, 26 rue d'Ulm 75248 Paris Cedex 05 France*
[4]*UMR 168, Institut Curie/CNRS, 26 rue d'Ulm 75248 Paris Cedex 05 France*
[5]*E.S.P.C.I, 10 rue Vauquelin, 75231 Paris Cedex 05, France*

(Received 18 September 2008; published 5 February 2009)

We propose a novel mechanism of cell motility, which relies on the coupling of actin polymerization at the cell membrane to geometric confinement. We consider a polymerizing viscoelastic cytoskeletal gel confined in a narrow channel, and show analytically that spontaneous motion occurs. Interestingly, this does not require specific adhesion with the channel walls, and yields velocities potentially larger than the polymerization velocity. The contractile activity of myosin motors is not necessary to trigger motility in this mechanism, but is shown quantitatively to increase the velocity. Our model qualitatively accounts for recent experiments which show that cells without specific adhesion proteins are motile only in confined environments while they are unable to move on a flat surface, and could help in understanding the mechanisms of cell migration in more complex confined geometries such as living tissues.

DOI: 10.1103/PhysRevLett.102.058103 PACS numbers: 87.10.−e, 83.80.Lz, 87.17.Jj

In addition to its obvious importance for biology, cell motility has motivated numerous studies in the physics community. Identifying simple mechanisms of self-motion of soft condensed matter is an important challenge for physics, cell biology, and biomimetic material technology. Sustained motion at low Reynolds number necessitates a constant energy input, and therefore an active system, that is a system driven out of equilibrium by an internal or an external energy source. The cell cytoskeleton is a striking example of such an active system. It is a network of long semiflexible filaments made up of protein subunits, interacting with other proteins such as motor proteins which use the chemical energy of adenosine triphosphate hydrolysis to exert active stresses that deform the network [1]. Other examples of active systems range from animal flocks to bacterial colonies [2,3] and vibrated granular media [4].

Modeling cell motility has inspired both experimentalists and theoreticians, who have now distinguished two main different mechanisms: polymerization (treadmilling) and contractility. Both polymerization induced motion [5,6] and contractility induced spontaneous flows have now been observed *in vitro* [1], and studied theoretically [7–9] and numerically [10]. In all models the key ingredients of motion are an energy input to compensate dissipation and sufficient adhesion or friction with a substrate to acquire momentum. The usual picture of cell locomotion is then as follows: the cell lamellipodium builds strong adhesion points with the substrate and pushes forward its membrane by polymerizing actin. At the back, the cell body contracts and breaks the adhesion points. In particular, the overall cell velocity is then limited by the actin polymerization rate (which, however, varies substantially between cell types), in agreement with available experimental data [11–13].

In a recent paper [14] (see also [15] for another cell type), it has been observed both *in vivo* and *in vitro* that mutant dendritic cells (DC) that are unable to produce active integrin complexes (adhesion proteins) display sustained motility in confined environments (tissues or synthetic polymeric gels), whereas they fail to move on flat two-dimensional substrates due to their reduced adhesion ability. These observations suggest the existence of an alternative mechanism of motility to the adhesion dependent picture outlined above. Here we propose a new, simple mechanism of motility which accounts for these observations. This mechanism is mainly powered by actin polymerization at the cell membrane, and strongly relies on geometric confinement. Interestingly, it does not necessitate strong specific adhesion, and yields velocities potentially larger than the polymerization velocity. This confinement induced motility mechanism is backed by *in vitro* experiments of DC motility in microfabricated channels [16] (see Fig. 1).

We first introduce our model in its minimal form of a polymerizing viscoelastic gel confined in a channel. We then refine this model to mimic motile cells in confinement. Finally, we show quantitatively that the contractile activity of myosin increases the velocity of motion.

The model, which relies on the hydrodynamic theory of active gels [7], is as follows. We consider an incompressible viscoelastic film confined in a bidimensional channel of width b. Note that this bidimensional geometry mimics the experimental conditions of channels of rectangular section (Fig. 1), and that the case of a cylindrical confining channel can be treated with minor modifications. The axes are defined with x along the channel and z across it. The confining walls are placed at $z = 0$ and $z = b$. We denote the components of the velocity of the gel by v_i, and the

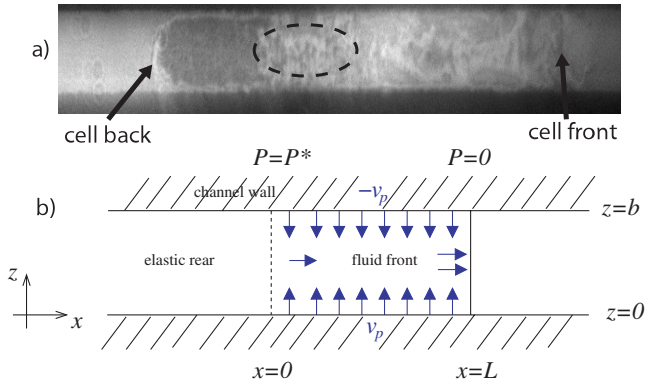

FIG. 1 (color online). (a) RICM image of a dendritic cell moving (to the right) in a channel of 4 μm width. The dark zone at the back of the cell (left) indicates a large contact of the membrane with the channel wall (independent of the nucleus, dotted line), and therefore a high normal constraint, compared to the front (right). The typical observed velocity reaches 12–15 μm/min in channels and 4–6 μm/min on a flat surface. (b) Channel geometry and model. The arrows show the flow direction.

strain rate by $u_{ij} = (\partial_i v_j + \partial_j v_i)/2$. We assume that the gel is described by a linear Maxwell model of viscoelasticity. The constitutive equation relating the strain rate to the deviatory stress tensor σ_{ij} is then written $2\eta u_{ij} = (1 + \tau \frac{D}{Dt})\sigma_{ij}$, where η is the shear viscosity, τ is a typical relaxation time, and D/Dt denotes the convective derivative. For dilute polymer gels, τ is very small and the gel behaves as a viscous fluid. At higher concentrations, or for more cross-linked gels, τ becomes very large and the gel behaves as an elastic medium. In what follows we assume that the gel is in either of the two regimes. For the sake of simplicity we assume here that the gel is incompressible, which means that τ depends on pressure P only. We define a critical pressure such that $\tau(P < P^*) = 0$ (viscous regime) and $\tau(P > P^*) = \infty$ (elastic regime). We next suppose that the gel is polymerized at the gel/substrate interface with speed $v_p \equiv v_z(x, z = 0) = -v_z(x, z = b)$ in the viscous regime, as depicted in Fig. 1. This is justified by the common observation of actin polymerization activators such as WASP proteins preferentially located along the cell membrane [11,17]. In the case of DCs, actin filaments can anchor perpendicularly to the cell membrane, forming structures called podosomes where polymerization takes place, therefore inducing an inward flow of actin as it is assumed in our model [18]. Finally, we assume viscous friction at the channel walls $z = 0$ and $z = b$, and write $\sigma_{xz} = \xi v_x$ where ξ characterizes the friction.

We now derive the dynamical equations of the system in the lubrication approximation ($b \ll L$ where L is the typical length of the system). In this limit the Reynolds number is small and the velocity field $v_i(x, z)$ can be obtained from the force balance $\partial_x P = \eta \partial_z^2 v_x$ and the condition of incompressibility $u_{xx} + u_{zz} = 0$. Defining the average velocity along the channel $v(x) = (1/b) \times \int_0^b v_x(x, z)dz$, we obtain the following Darcy's law:

$$v(x) = -\frac{b^2}{12\eta}\left(1 + \frac{6\eta}{b}\xi^{-1}\right)\frac{dP}{dx}. \quad (1)$$

Including the depolymerization of the gel k_d, mass conservation of the gel reads $\frac{dv}{dx} = 2v_p/b - k_d$, which gives in turn

$$\frac{d}{dx}\left[(1 + \tilde{\xi}^{-1})\frac{dP}{dx}\right] = \frac{12\eta(2v_p - bk_d)}{b^3}, \quad (2)$$

where v_p and the nondimensional friction $\tilde{\xi} \equiv \xi b/6\eta$ can be *a priori* functions of P and x.

Two boundary conditions are needed to determine the pressure profile $P(x)$. We neglect the friction with the surrounding fluid in the channel and set the pressure at the leading edge, which is assumed to coincide with the point $x = L$, as $P(L) = 0$, which gives the first boundary condition. Note that if the pressure at the leading edge is finite due to an external force, our results apply with an unimportant shift in the pressure field. We look for stationary states with broken symmetry and positive velocity and therefore the pressure is a decreasing function of x. We then argue that if the system is large enough, there exists a traveling front of gel of length L in the fluid phase, traveling at velocity V. The back boundary of this front fluid part coincides with the point $x = 0$ where the pressure reaches the threshold P^*, behind which is a growing elastic part. Such a denser elastic region at the back of DCs, called the uropod, is indeed well reported [19], and is characterized by a higher concentration of cross-linkers. As the velocity of the elastic part should be zero one has $v(0) = 0 = \frac{dP}{dx}|_{x=0}$, giving the second boundary condition which allows the explicit calculation of the pressure field. The self-consistent condition $P(0) = P^*$ gives in turn an equation enabling the calculation of the length L of the fluid front. We then write that the velocity V of the front is given by the calculated velocity of the flow plus the polymerization velocity at the leading edge $v(L) + v_p(L)$. We stress that the flow velocity is *forward*, i.e., in the same direction as the moving leading edge. Note that the length L of the fluid front is constant, which necessitates that the elastic-fluid boundary moves at the same velocity V.

Qualitatively, the value of the length L is dictated by the steepness of the pressure gradient, and therefore by the friction $\tilde{\xi}$. If $\tilde{\xi}$ is small, then only very long fluid fronts can move. We show now quantitatively that the coupling of $\tilde{\xi}$ with the pressure field actually enables short fluid fronts to move even with a low bare friction. The key ingredients are as follows. Following [20] we argue that the friction coefficient $\tilde{\xi}$ depends on the normal constraint in the case of a polymeric gel. Indeed qualitatively a high normal constraint increases the attachment rate of polymers onto the channel walls by lowering the entropic barrier, and decreases the detachment rate. It is shown in [20] that in the regime of moderate tangential speed, one has

$\tilde{\xi} = \tilde{\xi}_0 e^{\beta(P-\sigma_{nn})}$, where in our geometry the normal stress $\sigma_{nn} = \sigma_{zz}$ for both walls at $z = 0$ and $z = b$. Next, following standard ratchet models [21], the polymerization speed at the cell membrane is assumed to depend on the normal constraint in the gel according to $v_p = v_p^0 e^{-\alpha(P-\sigma_{zz})}$. These assumptions make Eq. (2) an autonomous equation for P, which is completed by the two boundary conditions discussed above.

To our knowledge, such an equation cannot be solved analytically in the general case. In the regime of small α (defined by $\alpha P^* \ll 1$), v_p can be taken as constant and an analytical approximation scheme can be proposed, which enables a discussion of the motility mechanism. We first neglect the elongational shear stress and write $\tilde{\xi} \approx \tilde{\xi}_0 e^{\beta P}$. This assumption underestimates the friction, and therefore the pressure field. Equation (2) can then be integrated and yields an implicit equation for the pressure field to lowest order P^0:

$$P^0 + \frac{\tilde{\xi}_0^{-1}}{\beta}(1 - e^{-\beta P^0}) = \frac{6\eta(2v_p^0 - bk_d)}{b^3}(L^2 - x^2). \quad (3)$$

This first expression P^0 gives a lower bound of the pressure field, and provides a satisfactory approximate (Fig. 2). To go further, we use $P^0(x)$ to determine the lowest order velocity profile $v_i^0(z)$ and calculate $\sigma_{zz}^0 = 2\eta\partial_z v_z^0$. Equation (2) is then resolved using this calculated numerical value of σ_{zz}^0, yielding the next order $P^1(x)$ which in turn can be used for further iterations. Using realistic values for the parameters corresponding to the actin cytoskeleton, used in [20,22], the procedure converges rapidly. Note that in the general case of any α, the first iteration giving $P^0(x)$ has to be performed numerically, and then the same procedure applies.

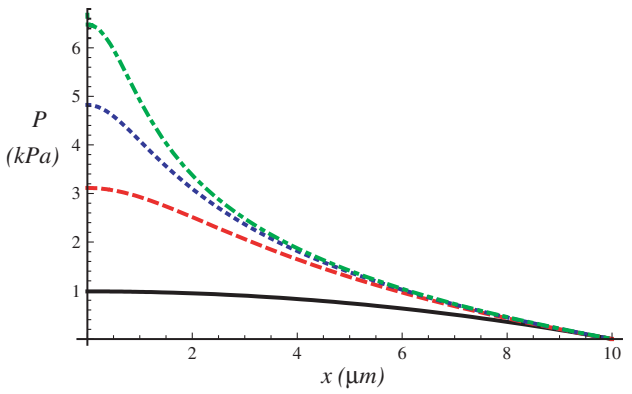

FIG. 2 (color online). Pressure profile. Dashed red: numerical value P^0 for $\beta = 1$ and $\alpha = 0.01$ kPa^{-1}; dotted blue: analytical expression Eq. (3) for $\beta = 1$, $\alpha = 0$; dot-dashed green: numerical value P^1 for $\beta = 1$, $\alpha = 0$; solid black: numerical value P^0 for $\beta = 0$, $\alpha = 0.01$ kPa^{-1}. Other parameters (estimates from [20,22]): $L = 10$ μm, $b = 1$ μm, $\eta = 10$ kPa s, $k_d = 0.1$ s^{-1}, $v_p^0 = 0.1$ μm s^{-1}, $\xi_0 = 0.1$ kPa s μm^{-1}. v_p^0 is taken as the speed of DCs on a surface which is expected to be the actin polymerization speed [13]. ξ_0 is taken as very small (lowest estimate in [20] which is 100-fold smaller than in keratocytes [7]) to mimic the low adhesion of integrin knockout DCs.

This mechanism therefore produces a *forward* flow which relies on a pressure buildup to P^* in the gel, here induced by confinement. It requires a minimal system size L given by taking $x = 0$ in Eq. (3). Interestingly, this can be obtained even for a very low bare friction coefficient ξ_0, since the exponential dependence of the friction on the pressure field permits the effective friction to reach large values for finite L, enabling motion.

On the other hand, Eq. (3) shows that L increases faster than linearly with b, indicating that this mechanism would not be significant in the case of a gel on a flat open substrate. In this case, which depicts the lamellipodium of a cell lying on a flat substrate (see [7]), the typical confining length b is large (of the order of the cell size), and the typical length L necessary to build a strong pressure gradient is very large ($L >$ cell size). As the pressure gradient in the cell is then much weaker than in the confined case, the friction with the substrate remains close to its bare value, yielding a much smaller momentum transfer with the substrate. Additionally, we then expect that the pressure remains below P^*, and that no elastic phase is formed, thus preventing forward flow. Without confinement, our model therefore suggests a *retrograde* flow, that is in the opposite direction to the moving leading edge, as previously modeled and observed for lamellipodia [7,23] on flat substrates. The flow direction, and therefore the direction of the pressure gradient in the gel, constitutes the main difference between the confinement induced mechanism of motility that we report here and the standard picture of cells lying on flat substrates.

Experimentally the pressure field can be quantified indirectly by measuring the effective contact area of the cell membrane using Reflection Interference Contrast Microscopy (RICM). Figure 1(a) [16] shows clearly that for a DC confined in a channel a larger contact area at the back of the cell is seen, indicating a backward pressure gradient in qualitative agreement with our theoretical prediction.

We now argue that this mechanism of confinement induced motility could be used by cells such as DCs to move in confined environments like channels. Extra hypotheses have to be added to the above model in order to more realistically capture the geometry of a moving cell. Instead of an open system, we assume now that the back edge is a thin slice where the gel is in its elastic regime, which mimics the uropod observed at the back of the cell. Additionally, we assume $\beta P^* \gg 1$ such that the friction of the uropod with the channel walls is very large, enforcing $v(0) = 0$. To conserve the total cell mass, we further assume that in the uropod the gel depolymerizes at the speed of the leading edge $V = v(L) + v_p(L)$ (which defines the over all speed of the cell). A high depolymerization rate in the uropod can be justified by the high pressure and a depletion of free actin monomers due to the forward flow. With these hypotheses, the model presented above

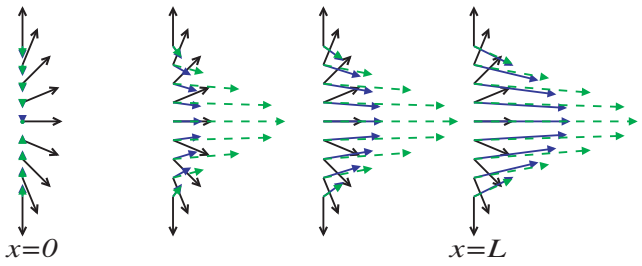

FIG. 3 (color online). Polarization (black) and flow velocity with (dashed green or gray) and without (blue or dark gray) myosin. Polarization arrows point in the direction of actin polymerization. The active term is taken as $\tilde{\zeta}(x)\Delta\mu = \tilde{\zeta}\Delta\mu(L-x)/L$ for $x > 0$ such that there are more myosins at the back of the cell.

mimics a cell moving in a channel with velocity V, and shows that the confinement induced motility mechanism can indeed be used by cells. Interestingly, for the parameter values used in Fig. 2 the front velocity is calculated to be $\sim 10\ \mu\mathrm{m}/\mathrm{min}$ which is close to the velocity that can be reached by DCs in collagen matrices [14] and in channels (up to 12–15 $\mu\mathrm{m}/\mathrm{min}$) [16] which significantly is larger than the polymerization velocity taken as the speed on a flat surface, 4–6 $\mu\mathrm{m}/\mathrm{min}$ [16,24].

Finally, we show that the coupling of the contractile effect of myosins with the normalized polarization field p_i of actin filaments (parametrized by its angle θ with the x axis) can also be taken into account. The polarization $\theta(z) = \theta_0 + \theta_1$ where $\theta_0 = -\frac{\pi}{2}(1 - \frac{2z}{b})$ is the static configuration which satisfies the normal anchoring boundary condition and θ_1 is assumed to be linear in v_p^0. Taking into account the active stress $\sigma_{ij}^{\mathrm{active}} = \tilde{\zeta}(x)\Delta\mu p_i p_j$ from [7], we obtain a perturbative solution around $v_p^0 = 0$ for the polarization and flow fields (shown in Fig. 3). Here it is also useful to consider the lubrication approximation $b \to 0$. To lowest order in this approximation, the polarization is given by its static configuration θ_0 and one obtains a generalized Darcy's law:

$$v(x) = -\frac{b^2}{12\eta}(1 + \tilde{\xi}^{-1})\frac{dP}{dx} - \frac{b\tilde{\zeta}(x)\Delta\mu}{4\pi\eta}, \qquad (4)$$

where $\tilde{\zeta}(x)\Delta\mu$ stands for the active coupling of myosins to actin filaments (see [7] for review), which is to linear order proportional to the myosin concentration. This equation shows that the contractile active stress induced by myosins ($\tilde{\zeta}\Delta\mu < 0$), increases the velocity of the actin flow, as shown in Fig. 3.

In conclusion, the motility mechanism of DCs in confined environments is strikingly different from the standard picture of cell motility on open flat substrates, and is well captured by our model of confinement induced motility. Importantly, this mechanism is widely independent of adhesion properties with the substrate, since the mechanism relies on an enhancement of friction due to a pressure buildup, and does not require specific adhesion proteins. In particular, this result is compatible with the experiments of [14], where it is found that integrin knocked out DCs are motile only in confined environments. Finally, the effect of myosin induced contractility can be taken into account, and yields a further enhancement of motility, in agreement with experiments [14,16].

[1] F. J. Nedelec, T. Surrey, A. C. Maggs, and S. Leibler, Nature (London) **389**, 305 (1997).
[2] C. Dombrowski *et al.*, Phys. Rev. Lett. **93**, 098103 (2004).
[3] Y. Hatwalne, S. Ramaswamy, M. Rao, and R. A. Simha, Phys. Rev. Lett. **92**, 118101 (2004).
[4] V. Narayan, S. Ramaswamy, and N. Menon, Science **317**, 105 (2007).
[5] A. Bernheim-Groswasser *et al.*, Nature (London) **417**, 308 (2002).
[6] V. Noireaux *et al.*, Biophys. J. **78**, 1643 (2000).
[7] K. Kruse *et al.*, Phys. Rev. Lett. **92**, 078101 (2004); Eur. Phys. J. E **16**, 5 (2005); F. Julicher *et al.*, Phys. Rep. **449**, 3 (2007).
[8] R. Voituriez, J. F. Joanny, and J. Prost, Europhys. Lett. **70**, 404 (2005); Phys. Rev. Lett. **96**, 028102 (2006).
[9] A. Zumdieck, R. Voituriez, J. Prost, and J. F. Joanny, Faraday Discuss. **139**, 369 (2008).
[10] D. Marenduzzo, E. Orlandini, M. E. Cates, and J. M. Yeomans, Phys. Rev. E **76**, 031921 (2007); J. Non-Newtonian Fluid Mech. **149**, 56 (2008).
[11] C. L. Clainche and M.-F. Carlier, Physiol. Rev. **88**, 489 (2008).
[12] T. D. Pollard and G. G. Borisy, Cell **112**, 453 (2003).
[13] J. A. Theriot and T. J. Mitchison, Nature (London) **352**, 126 (1991).
[14] T. Lämmermann *et al.*, Nature (London) **453**, 51 (2008).
[15] S. E. Malawista and A. de Boisfleury Chevance, Proc. Natl. Acad. Sci. U.S.A. **94**, 11 577 (1997).
[16] The experimental protocol will be published elsewhere.
[17] B. Alberts, *Molecular Biology of the Cell* (Garland Science, New York, 2002), 4th ed.
[18] Y. Calle, S. Burns, A. J. Thrasher, and G. E. Jones, Eur. J. Cell Biol. **85**, 151 (2006).
[19] J. M. Serrador, M. Nieto, and F. Sánchez-Madrid, Trends Cell Biol. **9**, 228 (1999).
[20] F. Gerbal, P. Chaikin, Y. Rabin, and J. Prost, Biophys. J. **79**, 2259 (2000).
[21] M. Dogterom *et al.*, Appl. Phys. A **75**, 331 (2002).
[22] A. C. Callan-Jones, J.-F. Joanny, and J. Prost, Phys. Rev. Lett. **100**, 258106 (2008).
[23] P. T. Yam *et al.*, J. Cell Biol. **178**, 1207 (2007).
[24] S. F. G. van Helden *et al.*, J. Immunol. **177**, 1567 (2006).